SCIENTIFIC REPORTS

OPEN

SUBJECT AREAS:
FERROELECTRICS AND MULTIFERROICS
ELECTRONIC DEVICES
SOLAR CELLS
OPTICAL MATERIALS AND STRUCTURES

Received
19 March 2013

Accepted
14 June 2013

Published
1 July 2013

Correspondence and requests for materials should be addressed to X.S. (xdsu@suda.edu.cn) or G.Z. (zouguifu@suda.edu.cn)

# Enlarging photovoltaic effect: combination of classic photoelectric and ferroelectric photovoltaic effects

Jingjiao Zhang[1], Xiaodong Su[1], Mingrong Shen[1], Zhihua Dai[1], Lingjun Zhang[1], Xiyun He[2], Wenxiu Cheng[2], Mengyu Cao[1] & Guifu Zou[1]

[1]Jiangsu Key Laboratory of Thin Films, Photovoltaic Research Institute of Soochow University & Canadian Solar Inc., Department of Physics, Soochow University, 1 Shizi street, Suzhou, 215006, P. R. China, [2]Key Laboratory of Inorganic Functional Materials and Devices, Shanghai Institute of Ceramics, Chinese Academy of Sciences, Shanghai 200050, People's Republic of China.

**Converting light energy to electrical energy in photovoltaic devices relies on the photogenerated electrons and holes separated by the built-in potential in semiconductors. Photo-excited electrons in metal electrodes are usually not considered in this process. Here, we report an enhanced photovoltaic effect in the ferroelectric lanthanum-modified lead zirconate titanate (PLZT) by using low work function metals as the electrodes. We believe that electrons in the metal with low work function could be photo-emitted into PLZT and form the dominant photocurrent in our devices. Under AM1.5 (100 mW/cm$^2$) illumination, the short-circuit current and open-circuit voltage of Mg/PLZT/ITO are about 150 and 2 times of those of Pt/PLZT/ITO, respectively. The photovoltaic response of PLZT capacitor was expanded from ultraviolet to visible spectra, and it may have important impact on design and fabrication of high performance photovoltaic devices based on ferroelectric materials.**

On the increasing needs of clean and renewable solar energy, researchers are continuously exploring novel materials and fundamentally investigating photoelectric conversion mechanisms for the better performance of photovoltaic (PV) devices[1–4]. Generally, two critical processes determined the photovoltaic effect: First, the electrical-charge carries such as electron-hole (*e-h*) pairs are generated by absorbing photons in active layers of the devices, i.e. semiconductors, dyes[5,6]. Second, the photo-generated *e-h* pairs are simultaneously separated by a built-in asymmetry potential formed in *p-n*/Schottky junction[7] or two electrodes with different work functions[8,9]. Usually, the performance of a photovoltaic device can be evaluated by measuring its open-circuit voltage ($V_{oc}$) and short-circuit current ($I_{sc}$), both are strongly depended on the light absorption ability of active layer, the strength and space of built-in field. Unfortunately, the performance of the semiconductor-based PV devices is mainly limited in two aspects: low $V_{oc}$ (typically below 1 V), and narrow space-charge region of a p-n junction[7,10]. Recent studies have revealed that the above two limitations can be broken in ferroelectric photovoltaic (FEPV) devices[11–13].

In a normal structure of electrode/ferroelectric/electrode, the ferroelectric could not only generate the photo-excited *e-h* pairs but also provide a polarization-induced internal electric field ($E_{pi}$, also called as depolarization electric field) to separate the photo-excited *e-h* pairs. Furthermore, electrodes can form two back-to-back Schottky barriers at the interfaces between the ferroelectric material and the electrode. The built-in fields ($E_{bi}$) due to Schottky barriers can deplete the ferroelectric layers. Generally, FEPV effect could create very high open-circuit voltage, sometimes over kV, but the short-circuit current density is very small even if under irradiation of ultraviolet (UV) irradiation[14]. To realize potential applications, such as light-electrical energy conversion, wireless energy transfer for a micro-electro-mechanical system (MEMS), the performance of FEPV devices must be improved significantly.

Therefore, many studies have been carried out to improve the FEPV properties by optimizing both ferroelectric and electrode materials. For instance, the number of *e-h* pairs will be increased significantly by using relative narrow band-gap $BiFeO_3$ ($E_g = 2.2$ eV) instead of wide band-gap ferroelectric[15,16], or incorporating narrow band-gap semiconductors such as $Ag_2O$ or $Cu_2O$ into $Pb(Zr,Ti)O_3$ (PZT) matrix[11,17]. In addition, the photocurrents and the photo-generated voltages can be further improved by modifying the configuration of electrodes in contact with ferroelectric materials[11,18].

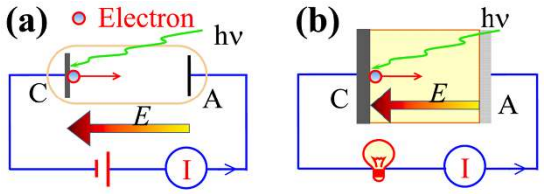


**Figure 1 | Illustrations of (a) a classic photoelectric diode, and (b) a proposal ferroelectric capacitor consisting of the ferroelectric layer and the photoemission electrode.** A: anode, C: cathode.

Electrons could be emitted from the surface of a metal into the vacuum under the irradiation of lights, where the photon energy is large than the work function of the metal. Such external photoelectric effect is the basis of classic photoelectric diodes as shown in **Fig. 1a**. Here, an applied field is necessary to collect excited electrons from the cathode. We noticed two facts in a classic photoelectric diode and a conventional ferroelectric photovoltaic cell: the cathode metals or alloys in the former have generally low work function. This allows high rate of electrons emitted into vacuum. On the other hand, the electrodes in the latter case are usually noble metals (i.e. Pt and Au) with high work function.

FEPV effects' studies are mostly based on an architecture of electrode/ferroelectric film/electrode, where the thickness of ferroelectric film is from several to hundreds of nanometers and the electrodes are noble metals (i.e. Pt and Au)[19–21]. Based on classic photoelectric effect theory, fewer electrons in Pt or Au can be excited by light irradiating due to a large barrier height existing at the interface which hinders the emission of electrons into the ferroelectrics. Furthermore, two interfaces between the ferroelectric film and top/bottom electrodes will result in a very complex physical picture of the device. For instance, the interface and the concomitant Schottky barriers can make ferroelectric layer partially or even totally depleted[22,23]. It is difficult to distinguish whether the $E_{pi}$ or $E_{bi}$ is dominant for the electron transport and photovoltaic properties. The open-circuit voltage (usually less than 1 V) of a ferroelectric film is influenced by the film's thickness[11,24].

In the present work, we report a novel concept of electrode/ferroelectric bulk/electrode capacitor combining classic photoelectric and ferroelectric effects, as shown in **Fig. 1b**. Here, the thickness of the ferroelectric pellet in hundreds of micrometers is much thicker than the thickness of interfaces. Therefore, the transport of carriers is dominant by $E_{pi}$ instead of the $E_{bi}$. In details, three types of cells were prepared in this work. The ferroelectric material is lanthanum-modified lead zirconate titanate (PLZT), and the top transparent electrodes for all samples are tin-doped indium oxide (ITO) facilitating light illumination through the top electrode. To clarify the role of photoelectric effect of metal electrodes on the FEPV cells, three different metals with work function of $\Phi_{Pt} = 5.5$ eV, $\Phi_{Ag} = 4.26$ eV, and $\Phi_{Mg} = 3.66$ eV were used as bottom electrodes, respectively.

Both short-circuit current ($I_{sc}$) and open-circuit voltage ($V_{oc}$) of the cells were improved remarkably under AM1.5 irradiation. Note that carriers in conventional ferroelectric cells are photo-generated *e-h* pairs. In our devices where one of the metal electrodes is of low work function, electron should be the majority carrier due to the contribution of emitted electrons from metal, in addition to the *e-h* pairs.

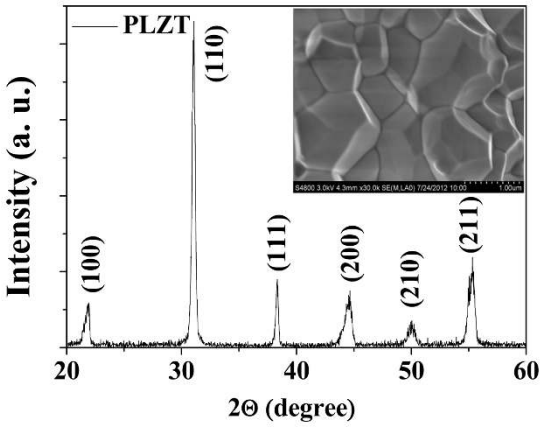


**Figure 2 | XRD pattern of PLZT ceramic bulk.** Insert: Cross-section SEM image of PLZT ceramic bulk.

## Results

Figure 2 shows XRD pattern of a pure $(Pb_{0.97}La_{0.03})(Zr_{0.52}Ti_{0.48})O_3$ (PLZT) pellet, illustrating single phase perovskite PZT structure with a lattice constant of a = b = 0.402 nm and c = 0.422 nm. The inset in Figure 2 is a cross-sectional SEM image of PLZT, displaying the polycrystalline feature of PLZT with grain size ~8–10 μm. It should be noted that an excess of 10% PbO added to account for loss of lead during processing, together with $La^{3+}$ substitution for $Pb^{2+}$, would ensure the final PLZT to be a *n*-type semiconductor[25,26]. This is very important to realize effective photoelectric effect to be discussed in this paper.

**Figure 3** shows ferroelectric hysteresis loops (*P–E*) of PLZT with different bottom electrodes. The inset schematically illustrates the device architecture. The measured remnant polarization ($P_r$) is around 45–50 $\mu C/cm^2$, close to those values reported in the literature[26]. The coercive field of the sample is ~20 kV/cm. Our experimental results imply that the measured ferroelectric properties of capacitors are not a strong function of metal electrodes.

To measure the photovoltaic properties of the PLZT cells, the devices with different electrodes were poled at an applied 1200 V for 15 minutes. A poling voltage well above the coercive voltage (~600 V) will ensure a full polarization of PLZT. In our experiment, we define the positive poling as the positive voltages applied to the bottom electrodes, i.e. Pt, Ag, and Mg. The negative poling is defined as the positive voltages applied to the top electrodes, i.e. ITO. With the light irradiated from either the top ITO or the bottom of metal electrodes, the open-circuit voltage and short-circuit current *vs.* measuring time were recorded by a self-made software through the Keithley 6517A consequently.

With irradiating light from the top (ITO), the time-dependent short-circuit current density ($J_{sc}$) and $V_{oc}$ were shown in **Figure 4**.

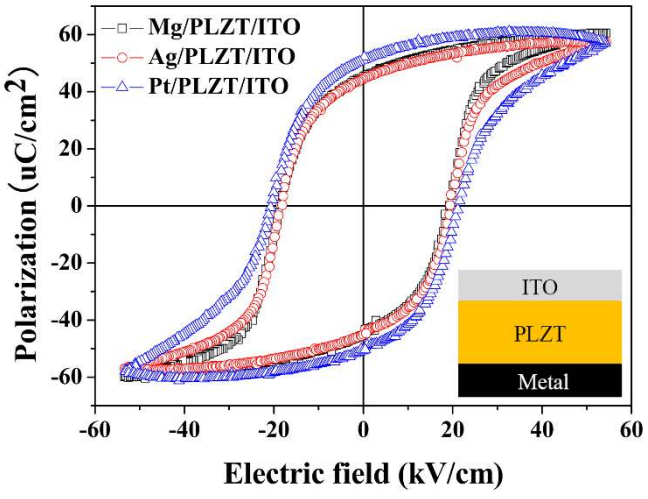


**Figure 3 | *P–E* hysteresis loops of the PLZT photodiodes with different bottom electrodes, Pt, Ag and Pt.** Insert: Illustration of the cross-section of a ferroelectric bulk capacitor.

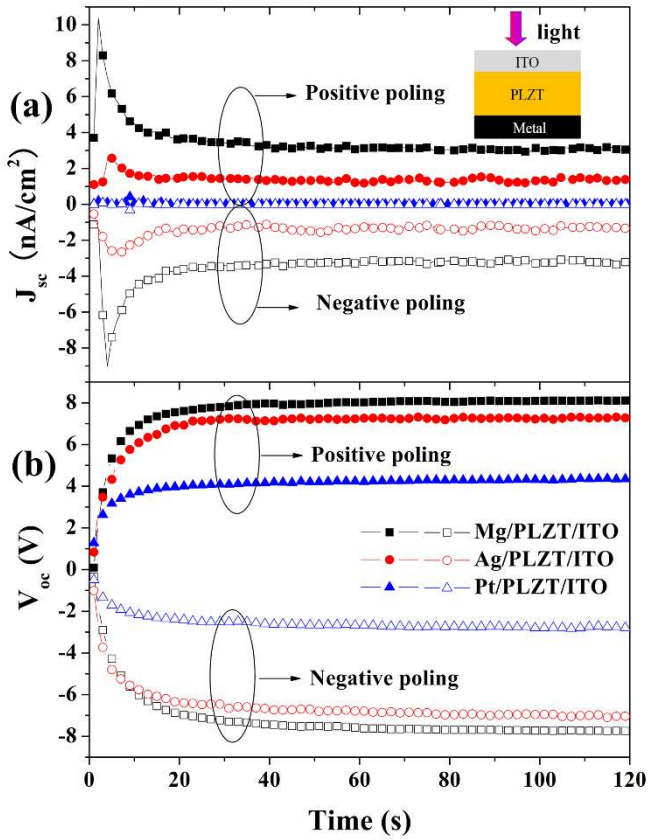


**Figure 4** | **(a) Short-circuit current density, and (b) open-circuit voltage *vs.* measuring time (Light irradiating from ITO).**

The observations can be summarized as: (1) both $J_{sc}$ and $V_{oc}$ strongly depend on the bottom metal electrodes. With decreasing of work function of metals ($\Phi_{Pt} > \Phi_{Ag} > \Phi_{Mg}$), both $I_{sc}$ and $V_{oc}$ increase dramatically ($J_{sc\text{-}Pt} < J_{sc\text{-}Ag} < J_{sc\text{-}Mg}$ and $V_{oc\text{-}Pt} < V_{oc\text{-}Ag} < V_{oc\text{-}Mg}$); (2) The variation of $J_{sc}$ and $V_{oc}$ on dependence of time follows the similar trend regardless of the bottom metal electrodes. Both $J_{sc}$ and $V_{oc}$ increase rapidly in the first several seconds. They then saturate at a certain value. Those transient responses by voltage and current may be due to the duration of the electrons transporting from top to bottom electrode, or caused by the pyroelectric effect to the current[27,28]; (3) Either in positive or in negative polarization, both $J_{sc}$ and $V_{oc}$ are almost symmetric. As mentioned early, we believe that with much thicker ferroelectric material, the carrier transport is controlled dominantly by the bulk ferroelectric effect rather than that of the localized Schottky barriers at interfaces.

We would like to point out that the short-circuit current and open-circuit voltage of Mg/PLZT/ITO are about 150 and 2 times respectively larger than those of Pt/PLZT/ITO. Although the mechanism of ferroelectric photovoltaic effect has not been fully understood, it has been speculated that ferroelectric photovoltaic effect is induced by the depolarization electric field which separates the photogenerated charge carriers[22,29]. Clarifying the relationship between $J_{sc}$ and $V_{oc}$ can help to understand above results. In a photovoltaic device, $J_{sc}$ arises from the movement of carries in the PLZT, but $V_{oc}$ comes from different chemical potential between the positive charges and negative charges piled on the top and bottom electrodes, respectively[30]. Similar to a *p-n* junction solar cell, the relationship between $J_{sc}$ and $V_{oc}$ can be expressed as[31]:

$$V_{oc} = \frac{nkT}{q}\ln\left(\frac{J_{sc}}{J_0}+1\right) \approx \frac{nkT}{q}\ln\left(\frac{J_{sc}}{J_0}\right)$$

Where $n$ is the ideality factor of the diode, $k$ is Boltzmann constant, $T$ is temperature in Kelvin, $q$ is the electron charge, and $J_0$ is reversal saturation current density of p-n junction. The much enhanced $J_{sc}$ will result in larger $V_{oc}$ if the $J_0$ is constant.

Usually, PLZT will exhibit photovoltaic effects under near-ultraviolet illumination due to its wide band-gap ($\lambda_c$ = 365 nm). We have noted that the fractional of light with photon energy greater than the band-gap of PLZT in our light source is about 5%, corresponding to a power density ~7.5 mW/cm$^2$. Therefore, such a large enhancement in $J_{sc}$ and $V_{oc}$ in Mg/PLZT/ITO cannot be simply attributed to the absorption of light by PLZT itself. The metal electrode must play a key role in determining the device performance. We expect that the electrons in metals can be excited by light irradiation and could be emitted into PLZT matrix, similar to the classic photoelectric effect. Under such circumstances, two kinds of carriers can contribute to the total photocurrent density $J_{sc}$: one is defined as $J_f$, generated from *e-h* pairs in *n*-type PLZT matrix, and another is $J_m$, generated from electrons in metal. Since the work function of Pt is high (5.5 eV), it is reasonable to ignore $J_m$. The $J_f$ is ~22 pA/cm$^2$ in a structure of Pt/PLZT/ITO. It is reasonable to assume that $J_f$ values is ~22 pA/cm$^2$ regardless of the electrodes used. Therefore, $J_m$ dominates the total photogenerated current in both Ag/PLZT/ITO ($J_{sc}$ = 1390 pA/cm$^2$) and Mg/PLZT/ITO ($J_{sc}$ = 3445 pA/cm$^2$) cells. The results imply that the much enhanced photovoltaic effect in the devices is from the photoelectric effect.

To further verify our concept, we measured photovoltaic properties of metal/PLZT/ITO cells by illuminating light from the metal side. As shown in **Figure 5**, the characteristics are similar to those shown in figure 4 but the values are much smaller. Since the thickness of metals (~100 nm) is thicker than the "skin depth", no light could penetrate into PLZT. The measured photocurrent and voltages should come from the electrons emitted from metal electrodes.

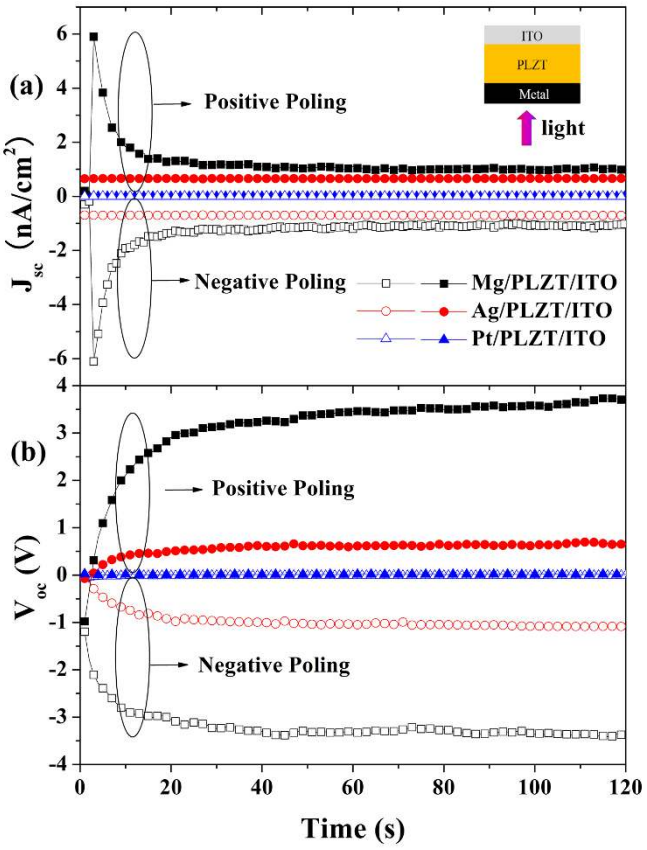


**Figure 5** | **(a) Short-circuit current density, and (b) open-circuit voltage *vs.* measuring time (Light irradiating from metal).**

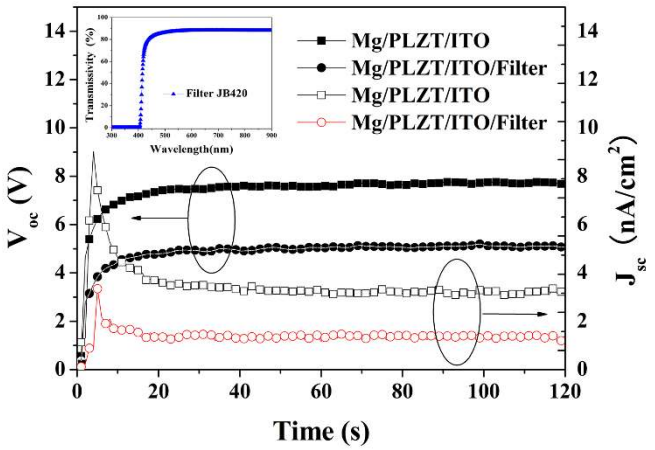


**Figure 6** | **Short-circuit current density and open-circuit voltage *vs.* measuring time for Mg/PLZT/ITO.**

Similar experiment was carried on Mg/PLZT/ITO. In this case, we inserted a filter JB420 between the light source and the sample during the measurement. This setup will allow the light with wavelength greater than 420 nm shine on the sample only. For PLZT with a band-gap of 3.4 eV, photocurrent can be generated by UV light at wavelengths shorter than 364 nm[32]. However, there still has considerable photocurrent even if there is no contribution from the photo-generated carriers in PLZT as presented in **Figure 6**. Our results reveal that the visible light could generate photocurrent in Mg/PLZT/ITO device, confirming that the photocurrent in Mg/PLZT/ITO can come from the emitted electrons in Mg electrode.

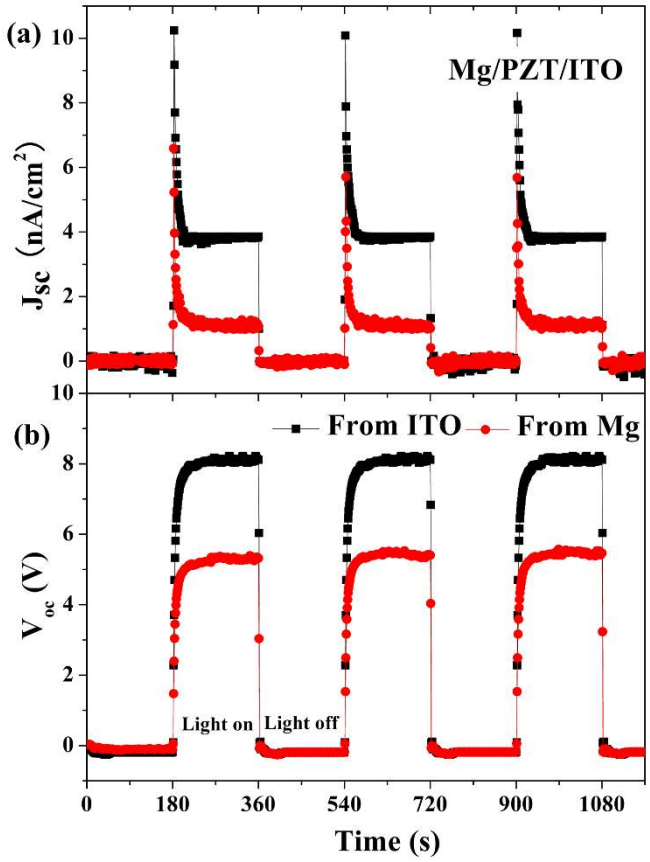


**Figure 7** | **Short-circuit current and open-circuit voltage *vs.* measuring time for Mg/PLZT/ITO.**

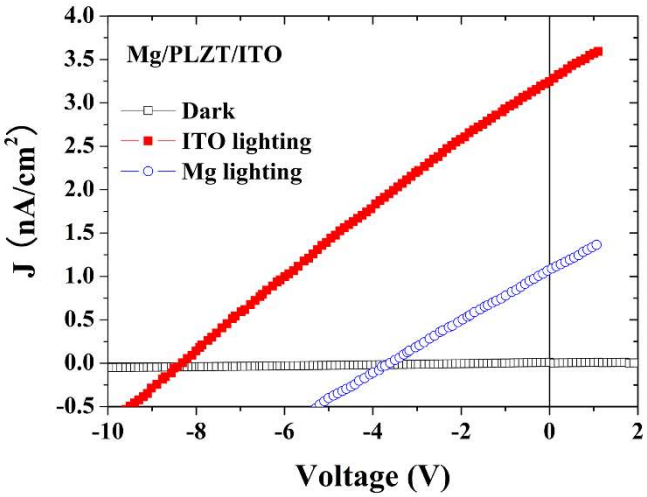


**Figure 8** | **J–V characteristics for Mg/PZT/ITO capacitor in dark and illumination conditions.**

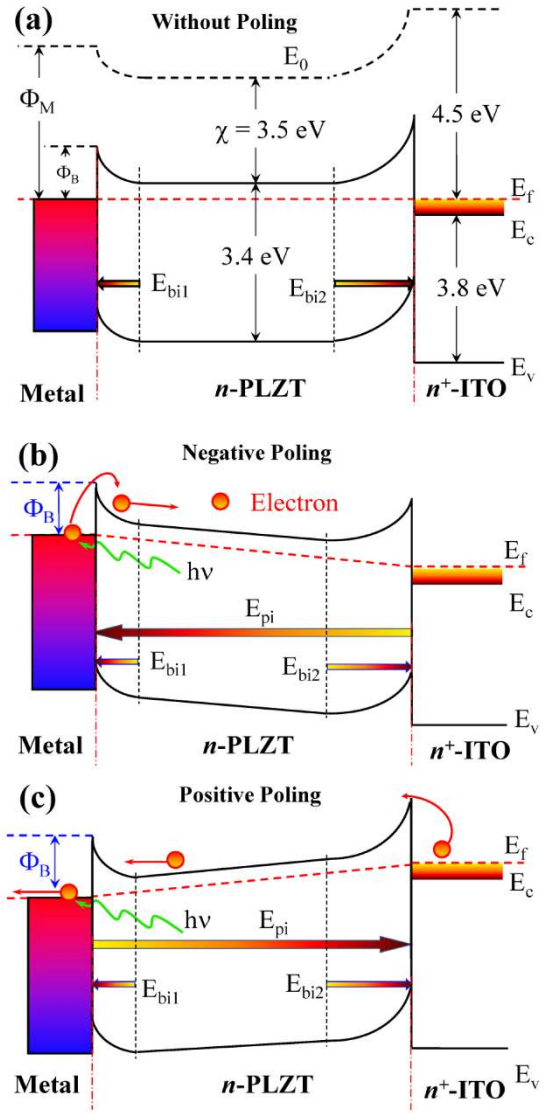


**Figure 9** | **Illustration of the energy band graph of Metal/PLZT/ITO, where $E_0$ is vacuum energy band, $E_c$ is conduct band, $E_v$ is valance band, and $E_f$ is Fermi level: (a) Before polarization, (b) and (c) after negative and positive polarization (the e-h pairs photo-generated in PLZT weren't indicated in graph).**

Table I | The data concerning different bottom metals

| Bottom electrode | Pt | Ag | Mg |
|---|---|---|---|
| $\Phi_M$, eV | 5.5 | 4.3 | 3.7 |
| $\Delta\Phi$, eV | −1 | 0.2 | 0.6 |
| $\Phi_B$, eV | 2 | 0.8 | 0.2 |
| Average $V_{oc}$, V (Top lighting) | +4.2/−2.8 * | +7.0/−6.7 | +8.1/−7.7 |
| Average $J_{sc}$, pA/cm$^2$ (Top lighting) | +22/−19 | +1390/−1384 | +3445/−3385 |
| Average $V_{oc}$, V (Bottom lighting) | +0.01/−0.01 | +0.6/−1.0 | +3.5/−3.5 |
| Average $J_{sc}$, pA/cm$^2$ (Bottom lighting) | +1/−6 | +656/−700 | +1210/−1295 |

*positive/negative poling.

**Figure 7** shows the temporal dependence of the photocurrent density and voltage of Mg/PZT/ITO cell. It is clear that there is no decay of photocurrent and voltage during 3 cycles of on-off the illumination light. **Figure 8** shows the dark and illuminated J-V curves for Mg/PZT/ITO cell. Under standard AM 1.5 illumination condition, $V_{oc}$ and $J_{sc}$ are 8.34 V and 3.25 nA/cm$^2$ for lighting from ITO, 3.58 V and 1.08 nA/cm$^2$ for lighting from Mg, respectively. Above results indicate a significant photovoltaic effect in Mg/PZT/ITO cell[33].

## Discussion

To explain our experimental results, we construct a simple model. **Figure 9** illustrates the energy band diagram of Metal/PLZT/ITO. The internal electric field in ferroelectric material can be classified as two independent components and written as: $E = E_{\rm bi} + E_{\rm pi}$, where $E_{\rm bi}$ is the net built-in field of two back-to-back Schottky contacts at the top and bottom interfaces. The $E_{bi}$ is the internal net potential ($\Delta\Phi = \Phi_{ITO} - \Phi_M$) in the device. If we take the work function of ITO as ~4.5 eV[34], the theoretical $\Delta\Phi$ is about −1, 0.2 and 0.6 eV for Pt, Ag and Mg, respectively. Considering the depletion layer thickness of Schottky contact is less than 200 nm[35] and the measured $V_{oc}$ is much larger than 1 V, the influence of localized $E_{bi}$ on the photovoltaic properties is less important than $E_{pi}$ which is across the whole region of PLZT.

The most important issue of this work is to clarify how the photoelectric effect of metal can improve the photovoltaic properties of a ferroelectric material. **Table I** list the most important parameters discussed in the article. Here the work function of PLZT is considered as 3.5 eV[11,36]. As the barrier height can be expressed as $\Phi_B = \Phi_M - \Phi_{PLZT}$, it is clear that the lower the work function of the metal is, the smaller of $\Phi_B$ is. Theoretically, the photon energy large than 2, 0.8 and 0.2 eV can enable to emit electrons from Pt, Ag and Mg into the PLZT, respectively. However, due to the reflection loss of light on the surface and interfaces, the existing of surface states[37], and the trapping of charge carriers in the defects[38], the final $J_{sc}$ is small. With the decrease of work function, electrons in Ag and Mg could be excited by light irradiation and are emitted into the PLZT. Different from the *e-h* pairs generated in PLZT, most of charge carriers in Ag/PLZT/ITO and Mg/PLZT/ITO are electrons. Compared with a conventional *p-n* junction diode, the recombination of *e-h* pairs in such capacitors can be reduced significantly due to that the photo-emitted electrons in PLZT are dominant.

In summary, we have demonstrated much enhanced photovoltaic effect in metal/PLZT/ITO cells by combining classic photoelectric and photovoltaic effects. By lowering the height of Schottky barrier at metal/PLZT interface, the electrons in metals could be emitted and contribute to the ferroelectric photovoltaic effect. By using a low work function metal as the electrode, i.e. magnesium, the short-circuit current density and open-circuit voltage of Mg/PLZT/ITO cell is about 150 and 2 times larger than those of Pt/PLZT/ITO cell under AM1.5 illumination. The photovoltaic response of PLZT capacitor was expanded from ultraviolet to visible spectra, and its performance could be further improved by optimizing the thickness and crystalline quality of ferroelectric materials as well as using an anti-reflection layer to reduce light losses.

## Methods

**Synthesis.** The detailed processing conditions to synthesize ceramic PLZT were described elsewhere[39]. After hot-pressing calcinations at 1240°C under a pressure 40 MPa, both sides of the sample (or pellet) were polished. The pellet was then cut into a size of 10 × 10 × 0.3 mm$^3$. Electrodes (ITO, Pt, Ag and Mg) with a thickness around 100 nm were deposited by radio-frequency (RF) magnetron sputtering at room temperature.

**Measurements.** The crystallographic structure of the PLZT samples was examined by X-ray diffraction (XRD, Rigaku D-MAX diffractometer with Ni filtered Cu Kα radiation). Ferroelectric hysteresis loops were recorded by using a ferroelectric analyzer (Radiant 609B-3, USA). Open-circuit voltage and short-circuit current were measured under illumination of a 150 W Xe bulb which is used to simulate the solar spectrum of AM 1.5(100 mW/cm$^2$)[20,40]. The thickness of electrodes was determined by scanning electron microscopy (SEM).


1. Semonin, O. E. *et al.* Peak External Photocurrent Quantum Efficiency Exceeding 100% via MEG in a Quantum Dot Solar Cell. *Science* **334**, 1530–1533 (2011).
2. Yang, S. Y. *et al.* Above-bandgap voltages from ferroelectric photovoltaic devices. *Nature Nanotechnology* **5**, 143–147 (2010).
3. Chen, T., Qiu, L., Yang, Z. & Peng, H. Novel solar cells in a wire format. *Chem. Soc. Rev.* **42**, 5031–5041 (2013).
4. Yang, Z. *et al.* Aligned carbon nanotube sheet for electrode of organic solar cell. *Adv. Mater.* **23**, 5636–5639 (2011).
5. Oh, J., Yuan, H. C. & Branz, H. M. An 18.2%-efficient black-silicon solar cell achieved through control of carrier recombination in nanostructures. *Nature Nanotechnology* **7**, 743–748 (2012).
6. O'Regan, B. & Grätzel, M. A low-cost, high-efficiency solar cell based on dye-sensitized colloidal $TiO_2$ films. *Nature* **353**, 737–740 (1991).
7. Wenham, S. R., Green, M. A., Watt, M. E. & Corkish, R. *Applied Photovoltaics* (Earthscan Ltd, 2006).
8. McGehee, D. G. Organic solar cells: Overcoming recombination. *Nature Photonics* **3**, 250–252 (2009).
9. Nalwa, H. S. *Handbook of Organic Electronics and Photonics* (American Scientific Publishers, 2008).
10. Qin, M., Yao, K. & Liang, Y. C. High efficient photovoltaics in nanoscaled ferroelectric thin films. *Appl. Phys. Lett.* **93**, 122904 (2008).
11. Yao, K., Gan, B. K., Chen, M. & Shannigrahi, S. Large photo-induced voltage in a ferroelectric thin film with in-plane polarization. *Appl. Phys. Lett.* **87**, 212906 (2005).
12. Huang, H. T. Solar energy: Ferroelectric photovoltaics. *Nature Photonics* **4**, 134–135 (2010).
13. Yang, X. L. *et al.* Enhancement of photocurrent in ferroelectric films via the incorporation of narrow bandgap $Ag_2O$ nanoparticles. *Adv. Mater.* **24**, 1202–1208 (2012).
14. Ichiki, M., Morikawa, Y., Nakada, T. & Maeda, R. AES and XPS study of PZT thin film deposition by the laser ablation technique. *Ceramics International* **30**, 1831–1834 (2004).
15. Yang, S. Y. *et al.* Photovoltaic effects in $BiFeO_3$. *Appl. Phys. Lett.* **95**, 062909 (2009).
16. Chen, B. *et al.* Effect of top electrodes on photovoltaic properties of polycrystalline $BiFeO_3$ based thin film capacitors. *Nanotechnology* **22**, 195201 (2011).
17. Cao, D. W. *et al.* High-Efficiency Ferroelectric-Film Solar Cells with an n-type $Cu_2O$ Cathode Buffer Layer. *Nano Lett.* **12**, 2803–2809 (2012).
18. Chen, F., Schafranek, R., Li, S., Wu, W. B. & Klein, A. Energy band alignment between Pb(Zr, Ti)$O_3$ and high and low work function conducting oxides-from hole to electron injection. *J. Phys. D: Appl. Phys.* **43**, 295301 (2010).
19. Maksymovych, P. *et al.* Dynamic conductivity of ferroelectric domain walls in $BiFeO_3$. *Nano Lett.* **11**, 1906–1912 (2011).
20. Cao, D. W. *et al.* Interface effect on the photocurrent: A comparative study on Pt sandwiched $(Bi_{3.7}Nd_{0.3})Ti_3O_{12}$ and $Pb(Zr_{0.2}Ti_{0.8})O_3$ films. *Appl. Phys. Lett.* **96**, 192101 (2010).

21. Choi, T., Lee, S., Choi, Y. J., Kiryukhin, V. & Cheong, S. W. Switchable ferroelectric diode and photovoltaic effect in $BiFeO_3$. *Science* **324**, 63 (2009).
22. Qin, M., Yao, K. & Liang, Y. C. Photovoltaic mechanisms in ferroelectric thin films with the effects of the electrodes and interfaces. *Appl. Phys. Lett.* **95**, 022912 (2009).
23. Cao, D. W. *et al.* Interface layer thickness effect on the photocurrent of Pt sandwiched polycrystalline ferroelectric Pb(Zr, Ti)$O_3$ films. *Appl. Phys. Lett.* **97**, 102104 (2010).
24. Pintilie, L., Alexe, M., Pignolet, A. & Hesse, D. $Bi_4Ti_3O_{12}$ ferroelectric thin film ultraviolet detectors. *Appl. Phys. Lett.* **73**, 342 (1998).
25. Afanasjev, V. P. *et al.* Polarization and self-polarization in thin $PbZr_{1-x}Ti_xO_3$ (PZT) films. *J. Phys.: Condens. Matter* **13**, 8755–8763 (2001).
26. Zeng, X. *et al.* Dielectric and ferroelectric properties of PZN-PZT ceramics with lanthanum doping. *J. Alloy. & Comp.* **485**, 843–847 (2009).
27. Glass, A. M., von der Linde, D. & Negran, T. J. Highvoltage bulk photovoltaic effect and the photorefractive process in $LiNbO_3$. *Appl. Phys. Lett.* **25**, 233 (1974).
28. Kholkin, A., Boiarkine, O. & Setter, N. Transient photocurrents in lead zirconate titanate thin films. *Appl. Phys. Lett.* **72**, 130 (1998).
29. Ichiki, M. *et al.* Photovoltaic properties of (Pb, La)(Zr, Ti)$O_3$ films with different crystallographic orientations. *Appl. Phys. Lett.* **87**, 222903 (2005).
30. Heyszenau, H. Electron transport in the bulk photovoltaic effect. *Phys. Rev. B* **18**, 1586–1592 (1978).
31. Wenham, S. R., Green, M. A., Watt, M. E. & Corkish, R. *Applied Photovoltaics* (Earthscan, 2007).
32. Scott, J. F. *Ferroelectric Memories* (Heidelberg: Springer, 2000).
33. Chen, B. *et al.* Tunable photovoltaic effects in transparent Pb($Zr_{0.53}$, $Ti_{0.47}$)$O_3$ capacitors. *Appl. Phys. Lett.* **100**, 173903 (2012).
34. Gassenbauer, Y. *et al.* Surface states, surface potentials, and segregation at surfaces of tin-doped $In_2O_3$. *Phys. Rev. B* **73**, 245312 (2006).
35. Boerasu, I., Pintilie, L., Pereira, M., Vasilevskiy, M. I. & Gomes, M. J. M. Competition between ferroelectric and semiconductor properties in Pb($Zr_{0.65}Ti_{0.35}$)$O_3$ thin films deposited by sol-gel. *J. Appl. Phys.* **93**, 4776–4783 (2003).
36. Nagaraj, B., Aggarwal, S., Song, T. K., Sawhney, T. & Ramesh, R. Leakage current mechanisms in lead-based thin-film ferroelectric capacitors. *Phys. Rev. B* **59**, 16022–16027 (1999).
37. Watanabe, Y. Electrical transport through Pb(Zr,Ti)$O_3$ *p-n* and *p-p* heterostructures modulated by bound charges at a ferroelectric surface: Ferroelectric *p-n* diode. *Phys. Rev. B* **59**, 11257–11266 (1999).
38. Gao, J. *et al.* Quantum dot size dependent J-V characteristics in heterojunction ZnO/PbS quantum dot solar cells. *Nano Lett.* **11**, 1002–1008 (2011).
39. Zhang, Y., Ding, A. L., He, X. Y., Cao, Z. P. & Yin, Q. R. Influence of Dy doping on microstructure of PLZT ceramics. *Key Engineering Materials* **280–283**, 1189–1192 (2005).
40. Zheng, F. G., Xu, J., Fang, L., Shen, M. R. & Wu, X. L. Separation of the Schottky barrier and polarization effects on the photocurrent of Pt sandwiched Pb($Zr_{0.20}Ti_{0.80}$)$O_3$ films. *Appl. Phys. Lett.* **93**, 172101 (2008).


## Acknowledgments

We are very grateful to Dr. Q.X. Jia from Los Alamos National Laboratory for enlightening discussions. This work was supported by the Natural Science Foundation of Jiangsu province under the Grant No. BK2012622, by the National Natural Science Foundation under the Grant No. 91233109, and by the Priority Academic Program Development of Jiangsu Higher Education Institutions (PAPD).

## Author contributions

X.S., Z.D., M.S. and L.Z. designed research; X.S., G.Z., Z.D., J.Z., M.C. and W.C. performed experimental and analyzed data; X.S., G.Z. and X.H. wrote the paper; and all authors reviewed the manuscript.

## Additional information

**Competing financial interests:** The authors declare no competing financial interests.

**How to cite this article:** Zhang, J. *et al.* Enlarging photovoltaic effect: combination of classic photoelectric and ferroelectric photovoltaic effects. *Sci. Rep.* **3**, 2109; DOI:10.1038/srep02109 (2013).